

# Heavy Flavor at the Large Hadron Collider in a Strong Coupling Approach

Min He<sup>a</sup>, Rainer J. Fries<sup>a</sup>, Ralf Rapp<sup>a</sup>

<sup>a</sup>*Cyclotron Institute and Department of Physics & Astronomy, Texas A&M University, College Station, TX 77843, USA*

---

## Abstract

Employing nonperturbative transport coefficients for heavy-flavor (HF) diffusion through quark-gluon plasma (QGP), hadronization and hadronic matter, we compute  $D$ - and  $B$ -meson observables in Pb+Pb ( $\sqrt{s}=2.76$  TeV) collisions at the LHC. Elastic heavy-quark scattering in the QGP is evaluated within a thermodynamic  $T$ -matrix approach, generating resonances close to the critical temperature which are utilized for recombination into  $D$  and  $B$  mesons, followed by hadronic diffusion using effective hadronic scattering amplitudes. The transport coefficients are implemented via Fokker-Planck Langevin dynamics within hydrodynamic simulations of the bulk medium in nuclear collisions. The hydro expansion is quantitatively constrained by transverse-momentum spectra and elliptic flow of light hadrons. Our approach thus incorporates the paradigm of a strongly coupled medium in both bulk and HF dynamics throughout the thermal evolution of the system.

*Keywords:* Heavy Flavor, Quark Gluon Plasma, Ultrarelativistic Heavy-Ion Collisions

*PACS:* 25.75.Dw, 12.38.Mh, 25.75.Nq

---

## 1. Introduction

Open heavy-flavor (HF) observables have developed into a key probe of the hot nuclear medium produced in ultrarelativistic heavy-ion collisions (URHICs) [1]. Once charm ( $c$ ) and bottom ( $b$ ) quarks are produced in primordial nucleon-nucleon collisions, their large masses suppress inelastic reinteractions, rendering their subsequent diffusion a quantitative tool to determine the thermalization timescale in the medium. Since this timescale appears to be comparable to the typical lifetime of the fireball formed in URHICs, the modifications imprinted on the final HF spectra provide a direct measure of the coupling strength to the medium.

The discovery [2, 3, 4] of the suppression of HF decay electrons in Au+Au collisions at the Relativistic Heavy Ion Collider (RHIC), accompanied by a remarkable elliptic flow, has become a benchmark of our understanding of the strongly coupled quark-gluon plasma (sQGP). The results imply substantial thermalization of heavy quarks due to frequent rescattering on medium constituents [5], with an estimated diffusion coefficient of  $\mathcal{D}_s \simeq 4/(2\pi T)$ . Several transport models have been developed to scrutinize these findings [5, 6, 7, 8,

9, 10, 11, 12, 13, 14, 15], differing in the microscopic interactions (both perturbative and non-perturbative), the modeling of the bulk medium evolution (fireballs, hydrodynamics and transport simulations), and the treatment of the HF kinetics (Boltzmann or Langevin simulations). With the advent of Pb+Pb collisions at the Large Hadron Collider (LHC), HF probes have entered a new era. The more abundant production of heavy quarks makes direct information on HF mesons available, allowing to disentangle charm and bottom spectra. The ALICE data corroborate a strong suppression and large elliptic flow of  $D$  mesons and non-photonic electrons in Pb+Pb ( $\sqrt{s_{NN}}=2.76$  TeV) collisions [16, 17, 18], but their simultaneous description is not easily achieved by existing theoretical models [19, 20, 21, 22, 23, 24, 25, 26, 27]. Non-prompt  $J/\psi$ , associated with  $B$ -meson decays, measured by CMS [28, 29] have opened a window on bottom-quark interactions with the medium. Finally, ALICE has presented first data on  $D_s$  mesons in Pb+Pb [30], which have been suggested as a particularly valuable probe to disentangle QGP and hadronic effects in the HF sector [15].

In the present paper we conduct a systematic comparison of our earlier constructed transport ap-

proach for open HF [14, 15] to available observables at the LHC. This approach implements a strong-coupling scheme in both micro- and macro-physics (i.e., HF transport and bulk evolution, respectively) of QGP and hadronic matter, and has been found to describe HF data at RHIC fairly well [14, 15]. Its building blocks are a quantitatively constrained hydrodynamic bulk evolution [31] into which HF transport is implemented using nonperturbative interactions for heavy quarks [32] and mesons [33] through QGP, hadronization [34] and hadronic phases of a nuclear collision. Since the diffusion processes are restricted to elastic interactions, it is of particular interest to study whether the much increased  $p_T$ -reach at the LHC requires additional physics not included in our approach, e.g., radiative processes. The predictive power of our calculations is retained by utilizing microscopic HF transport coefficients without  $K$ -factors. For the application to LHC we have refined our earlier reported results [21] with improved heavy-quark (HQ) baseline spectra and fragmentation in  $pp$  collisions, an update of the HQ  $T$ -matrix by including the gluonic sector, and a revised tune of the hydrodynamic model to bulk observables.

In the following, we first briefly review our non-perturbative diffusion framework emphasizing the updated inputs (Sec. 2). We then present comprehensive HF results for  $D$ ,  $D_s$ ,  $B$  mesons and decay electrons in Pb+Pb (2.76 TeV), and compare them to available data (Sec. 3). We summarize in Sec. 4.

## 2. Non-Perturbative HF Transport

Our formalism for HF transport through QGP, hadronization and hadronic phase has been introduced in Ref. [14]. We here recollect its main components and elaborate on updated inputs adequate for the phenomenology at LHC.

We compute the space-time evolution of the heavy-quark (-meson) phase-space distribution in the QGP (hadronic matter) using the Fokker-Planck (FP) equation, implemented via Langevin dynamics [35]. The FP equation follows from the Boltzmann equation through a second-order expansion in the momentum transfer,  $k$ , which is justified for HF momenta satisfying  $p^2 \sim m_Q T \gg T^2 \sim k^2$  ( $m_Q$ : HQ mass); the pertinent Einstein equation has been verified for nonperturbative interactions in Ref. [36]. The FP equation encodes the diffusion properties in well-defined transport coefficients

which can be computed from in-medium scattering amplitudes without the notion of a cross section [35].

In the QGP, the thermal relaxation rates,  $A(p, T)$ , for heavy quarks are taken from a thermodynamic  $T$ -matrix approach [32], which utilizes input potentials from thermal lattice QCD (lQCD), properly corrected for relativistic effects and consistent with HF spectroscopy in vacuum. In the QGP, we focus on the results using the internal energy, as the pertinent  $T$ -matrices lead to better agreement with the (independent) thermal lQCD “data” for quarkonium correlators and HQ susceptibilities [32, 37]. In our previous studies [14, 15, 21], nonperturbative HQ scattering off light quarks was supplemented with perturbative scattering off gluons; here, we replace the latter by the recently calculated HQ-gluon  $T$ -matrices [38], with the same lQCD potentials as for heavy-light quark interactions. This improvement leads to a ca. 25% increase of the total HQ relaxation rate. In addition, we allow for a further increase of  $\sim 20\%$  to represent the uncertainty when going from the HQ internal energies of Ref. [39] (used in our previous calculations) to those of Ref. [40], cf. Ref. [32]. The resulting HQ relaxation rates are enhanced over leading-order perturbative calculations [41] (with  $\alpha_s=0.4$ ) by up to a factor of  $\sim 5$  at low momenta and temperatures close to  $T_c$ . This enhancement is caused by near-threshold resonance structures which develop close to  $T_c$ ; it is reduced at higher  $T$  (e.g., to a factor of 2.5-3 at  $2T_c$ ) and at higher momenta where the perturbative results are approached. This dynamical 3-momentum dependence will be relevant in the  $D$ -meson nuclear modification factor discussed below. The resulting HQ spatial diffusion coefficient  $\mathcal{D}_s = T/(m_Q A(p=0, T))$  turns out to be quite comparable to quenched lQCD data [42, 43].

Around a pseudo-critical temperature of  $T_{pc}=170$  MeV, heavy quarks are hadronized into HF hadrons using the resonance recombination model (RRM) [34], with  $p_t^Q$ -dependent rates taken from the in-medium  $T$ -matrix. For simplicity, we here neglect the effects of a finite recombination time window [15] which could reduce the final  $D$ -meson  $v_2$  by up to 10%. The “left-over” quarks are fragmented (see below). In the RRM part of the  $D$  and  $B$  spectra, we account for the difference of hadro-chemistry in AA and  $pp$  collisions as in Ref. [15]; most notably, the strangeness enhancement in AA enhances  $D_s$  and  $B_s$  production, thereby slightly reducing the fraction of charm in

$D$  and bottom in  $B$  mesons.

In hadronic matter, the diffusion of  $D$  and  $B$  mesons is continued with transport coefficients calculated from elastic scattering amplitudes off pions, kaons, etas, anti-/nucleons and anti-/deltas [33].

For the space-time evolution of the medium in Pb+Pb( $\sqrt{s_{NN}}=2.76$  TeV), within which HF particles diffuse, we have retuned the ideal AZHYDRO code [44]. As before, we employ a lQCD equation of state (EoS) [45, 46] with pseudo-critical deconfinement temperature of  $T_{pc} = 170$  MeV, matched to a hadron resonance gas EoS with chemical freeze-out at  $T_{ch} = 160$  MeV. Our update pertains to initial conditions for which we use the Glauber model as in Ref. [47] with an initial time of  $0.4$  fm/ $c$ , without initial flow nor fluctuations. This yields a softer expansion than the one adopted in our previous LHC HF predictions [21], while the measured charged-hadron  $p_T$  spectra [48] and inclusive (low- $p_T$ ) elliptic flow [49],  $\langle v_2 \rangle$ , at kinetic freeze-out,  $T_{kin} = 110$  MeV, are fairly well reproduced, cf. Fig. 1. We believe that the inclusive  $v_2$  of charged hadrons, as a measure of the total bulk momentum anisotropy, provides a suitable calibration for the calculation of the HF elliptic flow acquired through the coupling to the medium.

Finally, we have to specify the initial conditions for the HQ spectra. We replace our previous PYTHIA tune with  $\delta$ -function fragmentation by a full FONLL calculation for HQ spectra (using the pertinent software package [50]) and fragmentation functions (FFs) according to Ref. [51] for charm (with parameter  $r = 0.1$ ), and Ref. [52] for bottom (with parameter  $\alpha = 29.1$ ). This framework successfully describes HF spectra in  $pp$  at collider energies [53, 54]. For applications in Pb+Pb we first generate HQ spectra for  $pp$  collisions at  $\sqrt{s}=2.76$  TeV and then fold in the EPS09 shadowing correction [16, 55] for charm quarks (but not for bottom). The resulting spectra are used as the initial condition for the Langevin simulations of HQ diffusion in the QGP, sampled via the test particle method. The FONLL fragmentation is also used in the hadronization process for  $c$  and  $b$  quarks which do not undergo resonance recombination at  $T_c$ .

### 3. HF Observables at LHC

We are now in a position to compute HF observables based on our final  $D$ - and  $B$ -meson spectra in

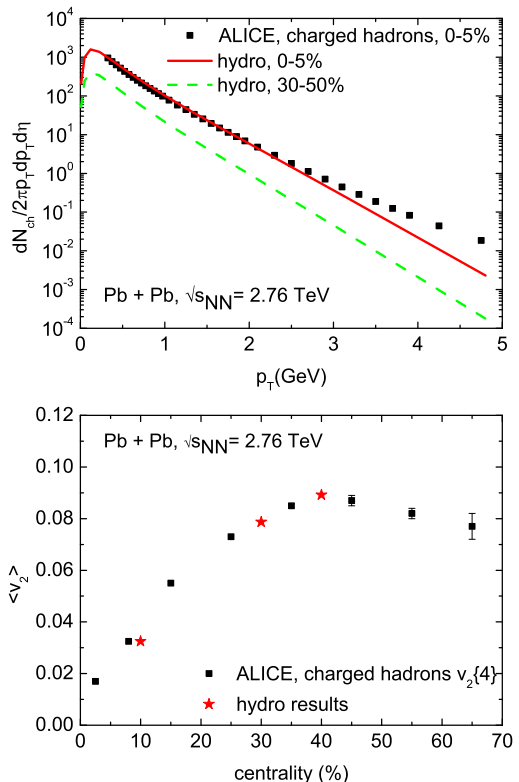


Figure 1: (Color online) Hydrodynamic fits of charged-hadron spectra and inclusive elliptic flow to ALICE data [48, 49] using our updated AZHYDRO tune.

Pb+Pb, i.e., their nuclear modification factor,

$$R_{AA}(p_T) = \frac{dN_{AA}/dp_T dy}{N_{coll} dN_{pp}/dp_T dy}, \quad (1)$$

and elliptic flow coefficient,

$$v_2(p_T) = \left\langle \frac{p_x^2 - p_y^2}{p_x^2 + p_y^2} \right\rangle, \quad (2)$$

where  $N_{coll}$  is the number of binary nucleon-nucleon collisions for the centrality bin under consideration.

Figure 2 displays the  $R_{AA}$  (0-20% centrality, upper panel) and  $v_2$  (30-50%, lower panel) of  $c$  quarks (just before hadronization) and  $D$  mesons (just after hadronization and at kinetic freezeout). Each quantity is shown as a band which encompasses the leading respective uncertainty, i.e., a shadowing reduction for  $R_{AA}$  (at 64-76% of the integrated yield), and the recombination probability for  $v_2$  (at 50-85% for the integrated  $c$ -quark fraction). Several features are noteworthy. The non-perturbative

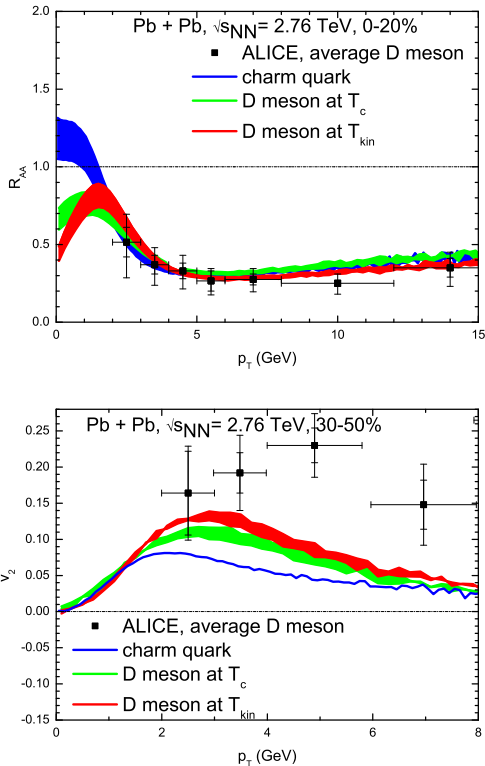


Figure 2: (Color online)  $R_{AA}$  (0-20% Pb+Pb, upper panel) and  $v_2$  (30-50% Pb+Pb, lower panel) for charm quarks and  $D$  mesons, compared to ALICE data [16, 17]. For  $R_{AA}$  ( $v_2$ ), the bands indicate uncertainties due to shadowing of charm production (the total charm-quark coalescence probability).

$c$ -quark diffusion in the QGP alone (via the  $T$ -matrix interaction) brings the  $R_{AA}^c$  already near the ALICE data [16] at intermediate and high  $p_T$ . Its increasing trend with  $p_T$ , resembling the data, is due to the dynamical momentum dependence of the relaxation rate. At low  $p_T$ ,  $R_{AA}^c$  increases monotonously down to  $p_T = 0$ , indicating the approach to thermalization. Upon resonance recombination with light quarks around  $T_c$  the monotonous increase transforms into a flow “bump” at  $p_T \simeq 1.5$  GeV in the  $D$ -meson  $R_{AA}$ , highlighting the role of recombination processes as further interactions contributing to thermalization [14]. Evidence of a flow bump has been observed at RHIC [56], corroborating the strong coupling of HF to the medium. At the LHC, low- $p_T$  ALICE data will thus provide another critical test of the degree of thermalization in general, and of model predictions to quantify the magnitude of the HF transport coefficients in particular. Interactions of  $D$  mesons in the hadronic

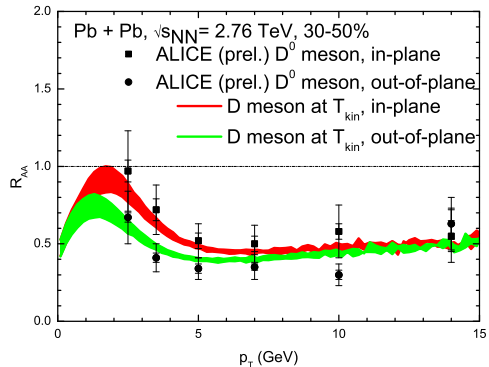


Figure 3: (Color online)  $D$ -meson in-plane versus out-of-plane  $R_{AA}$  for 30-50% centrality, compared to ALICE data [57]. The bands indicate shadowing uncertainties.

phase have a rather small effect on their final  $R_{AA}$ .

The situation is somewhat different for the elliptic flow. The combined effect of hadronization and hadronic diffusion increases the peak value of the final  $D$ -meson  $v_2$  by  $\sim 75\%$  over the QGP induced  $c$ -quark  $v_2$ . On the one hand, this is due to the bulk- $v_2$  taking a few fm/ $c$  to build up, and, on the other hand, due to the small spatial diffusion coefficient,  $\mathcal{D}_s \simeq 3\text{-}4/(2\pi T)$ , around  $T_{pc}$  (on both QGP and hadronic side). The prominent role of resonance recombination as an interaction driving HF toward equilibrium is once again apparent. This increase in  $v_2$ , which at the same time affects the  $R_{AA}$  relatively little, appears to be an important ingredient to simultaneously describe the ALICE data for *both* observables. Our calculation comes close to the combined  $D$ -meson  $v_2$  data from ALICE [17] up to  $p_T \simeq 4$  GeV, while it falls below above. This is reiterated by comparing our results to the in- vs. out-of-plane  $R_{AA}$  data [57]: the splitting tends to be underestimated at high  $p_T$ , cf. Fig. 3. In fact, the suppression observed in the  $R_{AA}$  at high  $p_T$  for the most central data sample (0-7.5%) is also significantly underestimated by our calculations, cf. Fig. 4. All of this points toward a lack of path-length dependence in our elastic quenching mechanism at high  $p_T$ , for which radiative energy loss is a natural candidate. Its rigorous implementation into a transport framework, including interference effects, currently remains a challenge.

The  $D_s$ -meson  $R_{AA}$  and  $v_2$  at low and intermediate  $p_T$  have recently been proposed as a remarkable signature to quantitatively probe the role of  $c$ -quark recombination and hadronic diffusion in

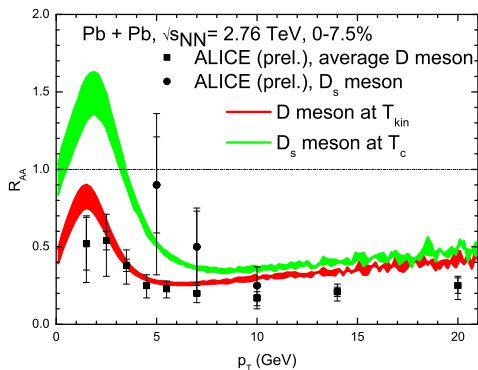


Figure 4: (Color online)  $D$ - versus  $D_s$ -meson  $R_{AA}$  for 0-7.5% central Pb+Pb, compared to ALICE data [30]. The bands indicate the charm-shadowing uncertainty.

URHICs [15]. An enhancement of the  $D_s$  over the  $D$   $R_{AA}$  has been predicted as a consequence of the well-established strangeness enhancement in URHICs (relative to  $pp$  collisions), realized through  $c$ -quark recombination with equilibrated strange quarks in the QGP [58]. Our predictions for LHC are compared to preliminary ALICE data [30] in Fig. 4, which indeed give a first indication of the proposed enhancement. At high  $p_T$ , fragmentation (universal in  $pp$  and Pb+Pb) leads to similar  $R_{AA}$ 's for  $D$  and  $D_s$  mesons, with a small splitting induced by an extra suppression of  $D$  mesons due to interactions in the hadronic phase; for  $D_s$  mesons hadronic rescattering is believed to be small and has been neglected in our calculations [15].

Next we turn to the bottom sector. Current information on  $B$ -meson spectra in Pb+Pb collisions is available through the CMS measurements of non-prompt  $J/\psi$ 's associated with  $B \rightarrow J/\psi + X$  decays [28, 29]. We calculate the  $B$ -meson  $R_{AA}$  for minimum bias Pb+Pb from a  $N_{\text{coll}}$ -weighted average over the three centrality bins 0-10%, 20-40% and 50-80%, see upper panel of Fig. 5. Since we do not introduce any shadowing correction for bottom, the uncertainty band in both  $R_{AA}$  and  $v_2$  refers to the integrated recombination probability of  $\sim 50$ -90%. At low  $p_T$ , the  $B$ -meson  $R_{AA}$  is close to 1 with a small flow ‘‘bump’’, i.e., a maximum at finite  $p_T \simeq 2$ -3 GeV, while the suppression for  $p_T \gtrsim 10$  GeV is rather flat at  $\sim 0.5$ . This is roughly consistent with the CMS non-prompt  $J/\psi$  data (we made no attempt to rescale the  $J/\psi$  momenta to reflect the parent  $B$ -meson momenta). The  $B$  mesons also acquire a sizeable  $v_2$ , reaching up to 7.5%, im-

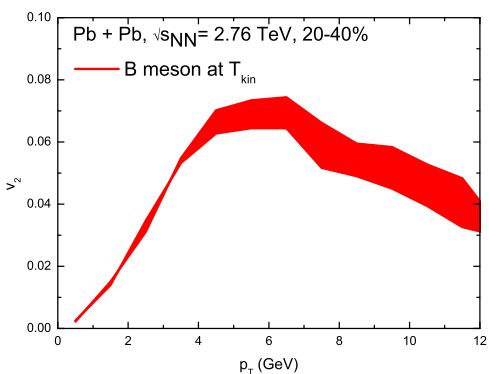
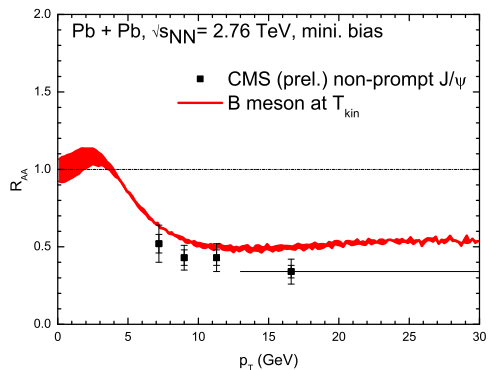


Figure 5: (Color online)  $B$ -meson  $R_{AA}$  (upper panel) and  $v_2$  (lower panel) in minimum-bias Pb+Pb. The bands indicate the uncertainty in the total  $b$ -quark coalescence probability (no shadowing is applied). The CMS data in the upper panel [28, 29] are for non-prompt  $J/\psi$  (associated with  $B$  decays) plotted vs. the  $J/\psi$   $p_T$  (no rescaling for  $B \rightarrow J/\psi + X$  decays is applied).

plying a significant approach to thermalization of bottom through diffusion and resonance recombination with light quarks. In contrast to charm, the bottom  $v_2$  peaks at a much higher  $p_T$ , which is in part a kinetic mass effect, but also due to a flatter momentum dependence of the  $b$ -quark relaxation rate [32, 38] and a coalescence probability function  $P_{\text{coal}}(p_t^Q)$  decreasing more slowly than for charm [14].

Finally, we compute HF electron observables from the semi-leptonic decays of  $D$  and  $B$  mesons. We first determine the bottom fraction of the single electrons in the  $pp$  baseline, which is illustrated in Fig. 6. With a bottom-to-charm cross section ratio of  $\sim 0.05$ , the pertinent ALICE data [59] can be reproduced. In our calculation the bottom contribution exceeds the charm one for electron momenta



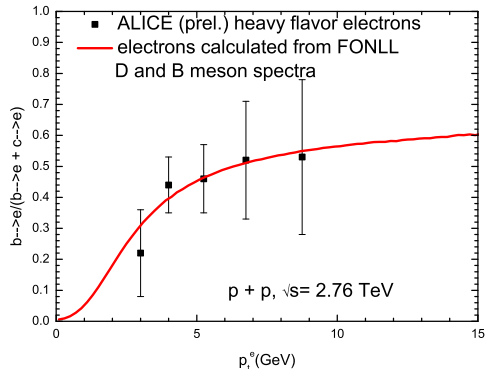


Figure 6: (Color online) Ratio of electrons from bottom to charm+bottom in  $pp$  collisions in comparison with ALICE data [59], assuming a total bottom-to-charm cross section ratio of  $\sim 0.05$ .

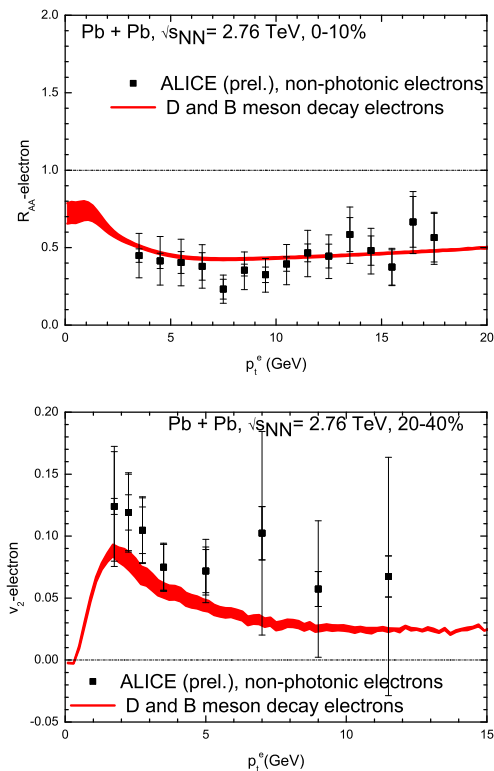


Figure 7: (Color online) Heavy-flavor electron  $R_{AA}$  and  $v_2$ , compared to ALICE data [18]. For  $R_{AA}$ ,  $\sim 50\%$  coalescence probability is applied for both  $D$  and  $B$  and the band indicates uncertainty in charm shadowing. For  $v_2$  the band indicates the uncertainty due to  $c$ - and  $b$ -quark coalescence probabilities of  $\sim 50\text{-}90\%$ .

above  $p_t^e \simeq 6$  GeV, although the ratio becomes quite flat. With this input we can convert our  $D$ - and  $B$ -meson observables computed above into single-electron ones, cf. Fig. 7 (as before, the bands indicate the leading uncertainties, i.e., charm shadowing for  $R_{AA}$  and charm/bottom integrated coalescence probabilities for  $v_2$ ). The ALICE data [18] for  $R_{AA}^e$  are reasonably well described while the calculated electron- $v_2$  appears to be somewhat low, especially toward higher  $p_t^e$ . In this regime the  $v_2^e$  is largely determined by the  $B$ -meson  $v_2$  as shown in the lower panel of Fig. 5. These features confirm the trends of the individual  $D$ - and  $B$ -meson observables.

#### 4. Summary

We have presented a comprehensive study of open HF probes in Pb+Pb collisions at  $\sqrt{s_{NN}} = 2.76$  TeV using a nonperturbative transport model which implements a strong-coupling approach of heavy quarks and hadrons into a hydrodynamically expanding medium. An overall fair description of the current data set from ALICE and CMS on the nuclear modification factor and elliptic flow of  $D$ ,  $D_s$ , non-prompt  $J/\psi$  from  $B$  decays and HF leptons emerges. In particular, our approach eases the tension between  $R_{AA}$  and  $v_2$  found previously, helped by a modest update of our QGP transport coefficient (now including nonperturbative HQ-gluon interactions) and a “softer” hydro expansion due to modified initial conditions. The key mechanism, however, first found in Ref. [5], is a strong HF coupling to the medium around  $T_{pc}$  (on both QGP and hadronic side), which includes the effects of resonance recombination. This insight corroborates that the QCD medium is most strongly coupled in the quark-to-hadron transition region of the phase diagram. At higher  $p_T$  our purely elastic treatment of HF-medium interactions seems to lack some strength and path-length dependence, which is not unexpected. On the other hand, more precise data at low and intermediate  $p_T$ , where we believe our approach to be most reliable, will allow for quantitative tests of the HF transport properties and their origin. Future plans include the study of HF baryons and more differential observables like HF correlations [60, 61, 62]. The inclusion of radiative effects will be required to improve the phenomenology at high momenta.

**Acknowledgments:** We are indebted to F. Riek and K. Huggins for providing the results for the HQ transport coefficients. This work was supported by the U.S. National Science Foundation (NSF) through CAREER grant PHY-0847538 and grant PHY-1306359, by the A.-v.-Humboldt Foundation, by the JET Collaboration and DOE grant DE-FG02-10ER41682, and by NSFC grant 11305089.

## References

- [1] R. Rapp and H. van Hees, in *Quark-Gluon Plasma 4* (R. Hwa and X.N. Wang, eds.), World Scientific (Singapore, 2010) 111 [arXiv:0903.1096 [hep-ph]].
- [2] B.I. Abelev *et al.* [STAR Collaboration], Phys. Rev. Lett. **98**, (2007) 192301; [Erratum-ibid. **106** (2011) 159902].
- [3] A. Adare *et al.* [PHENIX Collaboration], Phys. Rev. Lett. **98** (2007) 172301.
- [4] A. Adare *et al.* [PHENIX Collaboration], Phys. Rev. C **84** (2011) 044905.
- [5] H. van Hees, V. Greco and R. Rapp, Phys. Rev. C **73** (2006) 034913.
- [6] G.D. Moore and D. Teaney, Phys. Rev. C **71** (2005) 064904.
- [7] B. Zhang, L. -W. Chen and C. -M. Ko, Phys. Rev. C **72** (2005) 024906.
- [8] H. van Hees, M. Mannarelli, V. Greco and R. Rapp, Phys. Rev. Lett. **100** (2008) 192301.
- [9] P.B. Gossiaux, R. Bierkanndt and J. Aichelin, Phys. Rev. C **79** (2009) 044906
- [10] Y. Akamatsu, T. Hatsuda and T. Hirano, Phys. Rev. C **79** (2009) 054907 .
- [11] S. Mazumder, T. Bhattacharyya, J.-e Alam and S.K. Das, Phys. Rev. C **84** (2011) 044901 .
- [12] J. Uphoff, O. Fochler, Z. Xu and C. Greiner, Phys. Rev. C **84** (2011) 024908.
- [13] W.M. Alberico, A. Beraudo, A. De Pace, A. Molinari, M. Monteno, M. Nardi and F. Prino, Eur. Phys. J. C **71** (2011) 1666.
- [14] M. He, R.J. Fries and R. Rapp, Phys. Rev. C **86** (2012) 014903.
- [15] M. He, R.J. Fries and R. Rapp, Phys. Rev. Lett. **110** (2013) 112301.
- [16] B. Abelev *et al.* [ALICE Collaboration], JHEP **1209** (2012) 112.
- [17] B. Abelev *et al.* [ALICE Collaboration], Phys. Rev. Lett. **111** (2013) 102301.
- [18] S. Sakai *et al.* [ALICE Collaboration], Nucl. Phys. A **904-905** (2013) 661c.
- [19] J. Aichelin, P.B. Gossiaux and T. Gousset, Acta Phys. Polon. B **43** (2012) 655.
- [20] J. Uphoff, O. Fochler, Z. Xu and C. Greiner, Phys. Lett. B **717** (2012) 430.
- [21] M. He, R.J. Fries and R. Rapp, Nucl. Phys. A **910** (2013) 409.
- [22] T. Lang, H. van Hees, J. Steinheimer and M. Bleicher, arXiv:1211.6912 [hep-ph].
- [23] W.M. Alberico, A. Beraudo, A. De Pace, A. Molinari, M. Monteno, M. Nardi, F. Prino and M. Sitta, Eur. Phys. J. C **73** (2013) 2481.
- [24] S. Cao, G.-Y. Qin and S.A. Bass, Phys. Rev. C **88** (2013) 044907.
- [25] N. Armesto, A. Dainese, C. A. Salgado and U. A. Wiedemann, Phys. Rev. D **71** (2005) 054027.
- [26] Y. He, I. Vitev and B. -W. Zhang, Phys. Lett. B **713** (2012) 224.
- [27] A. Buzzatti and M. Gyulassy, Phys. Rev. Lett. **108** (2012) 022301.
- [28] S. Chatrchyan *et al.* [CMS Collaboration], JHEP **1205** (2012) 063.
- [29] CMS Collaboration, CMS-PAS-HIN-12-014.
- [30] G.M. Innocenti *et al.* [ALICE Collaboration], Nucl. Phys. A **904-905** (2013) 433c.
- [31] M. He, R.J. Fries and R. Rapp, Phys. Rev. C **85** (2012) 044911.
- [32] F. Riek and R. Rapp, Phys. Rev. C **82** (2010) 035201.
- [33] M. He, R.J. Fries and R. Rapp, Phys. Lett. B **701** (2011) 445.
- [34] L. Ravagli and R. Rapp, Phys. Lett. B **655** (2007) 126.
- [35] M. He, H. van Hees, P.B. Gossiaux, R.J. Fries and R. Rapp, Phys. Rev. E **88** (2013) 032138.
- [36] H. van Hees and R. Rapp, Phys. Rev. C **71** (2005) 034907.
- [37] F. Riek and R. Rapp, New J. Phys. **13** (2011) 045007.
- [38] K. Huggins and R. Rapp, Nucl. Phys. A **896** (2012) 24.
- [39] O. Kaczmarek and F. Zantow, Phys. Rev. D **71** (2005) 114510; O. Kaczmarek, PoS **CPOD07** (2007) 043.
- [40] P. Petreczky and K. Petrov, Phys. Rev. D **70** (2004) 054503.
- [41] B. Svetitsky, Phys. Rev. D **37** (1988) 2484.
- [42] H.T. Ding *et al.* J. Phys. G **38** (2011) 124070.
- [43] D. Banerjee, S. Datta, R. Gavai and P. Majumdar, Phys. Rev. D **85** (2012) 014510.
- [44] P.F. Kolb and W. Heinz, In \*Hwa, R.C. (ed.) et al.: Quark gluon plasma\* 634-714, [nucl-th/0305084].
- [45] S. Borsanyi *et al.*, JHEP **1011** (2010) 077.
- [46] A. Bazavov *et al.*, Phys. Rev. D **85** (2012) 054503.
- [47] Z. Qiu, C. Shen and U. Heinz, Phys. Lett. B **707** (2012) 151.
- [48] K. Aamodt *et al.* [ALICE Collaboration], Phys. Lett. B **696** (2011) 30.
- [49] R. Snellings *et al.* [ALICE Collaboration], J. Phys. G **38** (2011) 124013.
- [50] M. Cacciari, S. Frixione and P. Nason, JHEP **0103** (2001) 006.
- [51] E. Braaten, K.-m. Cheung, S. Fleming and T.C. Yuan, Phys. Rev. D **51** (1995) 4819.
- [52] V.G. Kartvelishvili, A.K. Likhoded and V.A. Petrov, Phys. Lett. B **78** (1978) 615.
- [53] M. Cacciari, P. Nason and R. Vogt, Phys. Rev. Lett. **95** (2005) 122001.
- [54] M. Cacciari, S. Frixione, N. Houdeau, M.L. Mangano, P. Nason and G. Ridolfi, JHEP **1210** (2012) 137.
- [55] K.J. Eskola, H. Paukkunen and C.A. Salgado, JHEP **0904** (2009) 065.
- [56] W. Xie *et al.* [STAR Collaboration], Nucl. Phys. A **904-905** (2013) 170c.
- [57] D. Caffarri *et al.* [ALICE Collaboration], Nucl. Phys. A **904-905** (2013) 643c.
- [58] I. Kuznetsova and J. Rafelski, Eur. Phys. J. C **51** (2007) 113.
- [59] M. Kweon *et al.* [ALICE Collaboration], arXiv:1208.5411 [nucl-ex].
- [60] X. Zhu *et al.*, Phys. Lett. B **647** (2007) 366.
- [61] X. Zhu, N. Xu and P. Zhuang, Phys. Rev. Lett. **100** (2008) 152301.
- [62] M. Nahrgang, J. Aichelin, P.B. Gossiaux and

K. Werner, arXiv:1305.3823 [hep-ph].